Articles

Allosteric Hammerhead Ribozyme TRAPs†

Donald H. Burke,*,‡ Nicole D. S. Ozerova,‡ and Marit Nilsen-Hamilton§

Department of Chemistry, Indiana University, Bloomington, Indiana 47405-7102, and Department of Biochemistry, Biophysics and Molecular Biology, Iowa State University, Ames, Iowa 50011

Received February 20, 2002

ABSTRACT: A new mode of allosteric regulation of nucleic acid enzymes is described and shown to operate effectively with hammerhead ribozymes. In the "TRAP" design (for targeted ribozyme-attenuated probe), a 3′ terminal "attenuator" anneals to conserved bases in the catalytic core to form the "off" state of the ribozyme. Binding of RNA or DNA to an antisense sequence linking the ribozyme and attenuator frees the core to fold into an active conformation, even though the antisense sequence itself does not interfere with the ribozyme. TRAP hammerheads based on the previously characterized HH8 ribozyme were shown to be activated more than 250-fold upon addition of the sense strand. RNA oligonucleotides were more effective activators than DNA oligos, consistent with the known relative helix stabilities (RNA−RNA > RNA−DNA). Oligonucleotides that directly paired with the attenuator gave up to 1760-fold activation. The magnitude of the activation was greater when the oligo was added prior to folding than if it was added during the cleavage reaction. The TRAP design requires no prior knowledge of (deoxy)ribozyme structure beyond identification of the essential core. Thus, this approach should be readily generalizable to other systems for biomedicine, sensor technology, and additional applications.

Since the discovery of natural endonucleolytic ribozymes, there has been a sustained effort to engineer both natural and in vitro-selected nucleic acid enzymes to display enhanced substrate specificities, turnover rates, stabilities against ribonucleases, and responsiveness to various modes of regulation. Most RNA-cleaving nucleic acid enzymes bind their substrates by forming a base-paired stem with an internal guide sequence (IGS)[1] complementary to nucleotides on both sides of the scissile bond. Aside from idiosyncratic sequence requirements at or adjacent to the cleavage site, RNA-cleaving enzymes can generally be designed to target a broad range of sequences through the appropriate choice of IGS.

The kinetic framework outlined for the hammerhead ribozyme (*1*) is typical of that displayed by many of the small RNA-cleaving nucleic acid enzymes. In the simplest hammerheads (Figure 1A), substrate binding via the IGS (k_1) is followed by target strand cleavage (k_2) and dissociation of the two cleaved fragments (branched pathway, not shown).

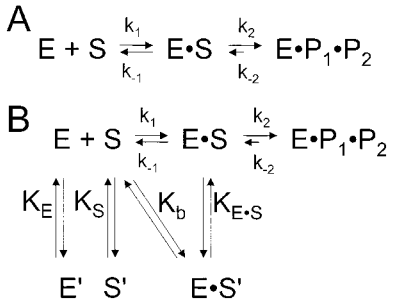

FIGURE 1: Kinetic framework for single-turnover RNA cleavage, adapted from ref *1*. (A) Simple scheme that applies to many RNA-cleaving nucleic acid enzymes. (B) Elaborated scheme for incorporation of additional kinetic steps that can become rate-limiting in certain cases. See the text for details.

This scheme can be expanded to include additional terms that reflect competition among alternative structures that hinder formation of the active E·S complex (Figure 1B). For example, self-structure within the enzyme (E′) may interfere with binding to the substrate (K_E). The native structure of the substrate (S′) may block access to the target cleavage site and association with the enzyme (K_S). After the IGS binds to the target, inactive conformations of the annealed enzyme−substrate complex (E·S′) may be stabilized relative to the active conformation ($K_{E·S}$), again slowing production of the active complex. Furthermore, alternative structures can be "on-pathway" if they are obligate intermediates en route to a productive E·S complex (such as the $K_b \rightarrow K_{E·S}$ pathway), or they can be "off-pathway" if they represent nonproductive detours. Variations of this kinetic scheme also

† The work was supported by a Beckman Young Investigator Award and NIH Grant AI45344 to D.H.B. and by DOE Grant DEA-01-P-043 to M.N.-H. This is journal paper J-19784 of the Iowa Agriculture and Home Economics Experiment Station, Ames, IA, Project 3529.

* To whom correspondence should be addressed. Telephone: (812) 856-4977. Fax: (812) 855-8355. E-mail: dhburke@indiana.edu.

‡ Indiana University.

§ Iowa State University.

[1] Abbreviations: TRAPs, targeted ribozyme-attenuated probes; IGS, internal guide sequence; E, enzyme; S, substrate; DNAzyme, deoxyribozyme; k_{obs}, observed kinetic rate constant; K_m, Michaelis−Menten constant; K_d, dissociation constant.

10.1021/bi0201522 CCC: $22.00
Published on Web 04/24/2002

apply to large catalytic RNAs. The group I self-splicing intron from *Tetrahymena thermophila*, for example, first binds its substrate via the IGS through Watson−Crick interactions to form the P1 helix, and then P1 docks into the core in a kinetically separable step (*2*). Structural rearrangements early in the folding process can also influence the overall catalytic rate (*3*).

There are many applications for which regulation of RNA-cleaving activity by an extrinsic factor would be desirable, including controlled cleavage of mRNA or viral RNA in cells and analyte detection on microarray chips. The expanded kinetic view outlined above offers many opportunities for introducing regulatory checkpoints that act as "molecular switches" prior to the chemical step. Ribozymes and deoxyribozymes (DNAzymes) have been engineered to respond to the binding of oligonucleotides (*4*−*9*) or other ligands (*10*−*19*). The "effectors" are thought either to shift the $K_{E\cdot S}$ equilibrium by converting nonproductive E·S′ complexes into productive E·S complexes or to shift the K_E equilibrium by releasing self-structure in the enzyme that prevents substrate binding.

In principle, any reversible perturbation of the precleavage equilibria can be exploited to impose regulation. Where RNA or DNA species act as positive regulators, the design strategy should ideally allow a wide range of sequences to be used as activators. However, several current designs for oligonucleotide-activated (deoxy)ribozymes either do not permit facile retargeting of the activating sequence or offer only modest stimulation by their target oligonucleotide. Specifically, the activating oligonucleotides often bind to sequences that participate directly in forming the inhibitory structure. As a result, re-engineering the activation specificity is restricted to oligonucleotides that are complementary to sequences that act in an inhibitory fashion. We hypothesized that a more generic regulation should be possible if the antisense function (binding to the activating species) and attenuation function (formation of the inhibitory species) were separated into distinct modules. Ribozymes that follow this design, known as TRAPs (for targeted ribozyme-attenuated probes), are shown here to be regulated by DNA or RNA oligonucleotides, even though the antisense binding site for the activating "sense" strand does not directly interfere with ribozyme activity.

EXPERIMENTAL PROCEDURES

Preparation of Oligonucleotides and Ribozymes. Transcription templates were synthesized as single-stranded DNA oligonucleotides using standard phosphoramidite chemistry by the Iowa State University DNA Sequencing and Synthesis Facility or by Integrated DNA Technologies (IDT). The synthetic coding strand was made double-stranded by PCR. One PCR primer (5′ GCT TAA TAC GAC TCA CTA TA 3′) contained a T7 RNA polymerase promoter (underlined). The other primer, chosen from among those shown in Figure 3A, defined the 3′ end of runoff transcripts from these templates. Double-stranded DNA was precipitated, resuspended in TE buffer [10 mM Tris-HCl (pH 8.0) and 1 mM EDTA], and transcribed in vitro (*20*) using T7 RNA polymerase purchased from Epicentre. RNA oligos used as the cleavage substrate or as activating effectors were synthesized by IDT. The substrate molecule was a 13-mer

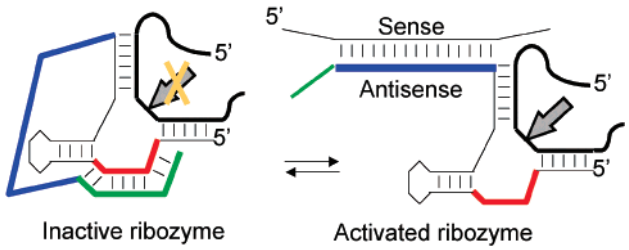

FIGURE 2: Schematic representation of TRAP design as applied to hammerhead ribozymes. Green and red lines correspond to strands that interact in the "closed", or "off" state (left side); blue is antisense. The cleavage site in the substrate strand (thick black line) is shown as a block arrow.

oligoribonucleotide that anneals to the IGS of the ribozymes as shown in Figure 3A. The substrate was 5′ end-labeled with [^{32}P]monophosphate using [γ-^{32}P]ATP (ICN) and T4 polynucleotide kinase from Epicentre. Uniformly radiolabeled transcripts and end-labeled substrate RNA were purified on denaturing (7 M urea) 12% polyacrylamide gels. Excised gel slices were crushed and soaked in 300 mM sodium acetate and 10 mM EDTA, filtered, ethanol precipitated, and resuspended in water prior to use.

Kinetics Assays. For the standard kinetics assays, 10 pmol of substrate was combined with 100 pmol of ribozyme in 90 μL of 50 mM Tris-HCl (pH 7.5), heated to 90 °C for 1 min, and then allowed to cool slowly to 25 °C for 5 min. If activating oligonucleotide was to be included in the cleavage reaction, 300 pmol was added prior to heating to 90 °C, unless otherwise indicated. An aliquot of 9 μL was taken prior to initiation as a "zero" time point, and then 9 μL of 100 mM $MgCl_2$ was added to give a final concentration of 10 mM to initiate the cleavage reaction. From the remaining 90 μL, aliquots of 10 μL each were taken at 15 s, 30 s, 45 s, 1 min, 2 min, 5 min, 10 min, 20 min, and 30 min. Reactions involving ribozymes HH8A.10 and HH8A.8 were much slower, and were extended to longer times (35 and 8 h, respectively), with correspondingly fewer aliquots at short time intervals. Aliquots were quenched with 10 μL of 50 mM EDTA, 8 M urea, 10% sucrose, 35% glycerol, 0.5% bromophenol blue, and 0.5% xylene cyanol (*21*). For experiments in which activating oligo was added after reaction for 1 h, the final concentrations of the activating oligo and magnesium were 1 and 8.65 mM, respectively. The inadvertently lower Mg^{2+} concentration is expected to decrease cleavage rates only slightly. Thus, while our estimate of oligo-mediated activation must be considered a lower bound, only minimal adjustment need be made for changes in Mg^{2+} concentration. Quenched aliquots were stored on dry ice and then resolved on 12% denaturing (7 M urea) polyacrylamide gels. Gels were dried and subjected to phosphorimaging analysis using the ImageQuant software from Molecular Dynamics. The fraction cleaved in each reaction was calculated as (counts in product band)/(counts in product band and substrate band). Experimental k_{obs} and half-life values were determined by plotting ln(fraction uncleaved) versus time and fitting a line through the initial values. Typically, four to six time points fell within the linear portion of the plot.

RESULTS

Attenuator Sequences Maintain HH8 in the "Off" State. The capacity to form alternative base-pairing patterns can

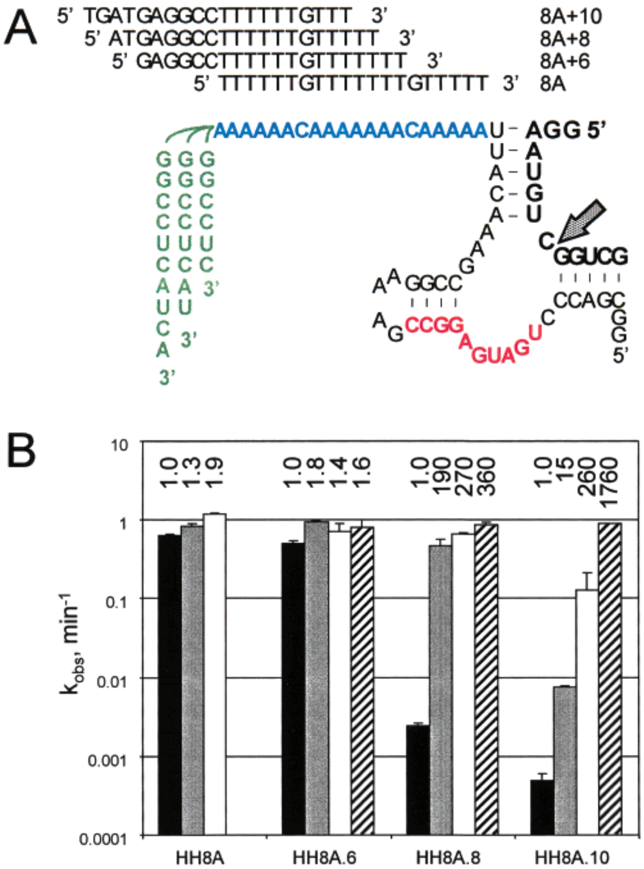

FIGURE 3: Structures and activities of HH8A and derivatives. (A) The 54-nucleotide ribozyme HH8A is shown annealed to a 13-nucleotide RNA substrate (bold). Cleavage at the site indicated with the block arrow yields two fragments, eight and five nucleotides in length. Following standard hammerhead designations, stem I is shown horizontally on the right, stem II is horizontal on the left, and stem III is vertical. Following the color scheme used in Figure 2, attenuator sequences used in constructs HH8A.6, HH8A.8, and HH8A.10 are shown in green appended to HH8A on the left-hand side, attenuator binding targets within the core are in red, and the 20-nucleotide antisense segment at the 3′ end of HH8A is shown in blue. Oligonucleotides used in PCRs to generate transcription templates and in RNA cleavage reactions to activate allosteric ribozymes are shown above the ribozyme. Oligonucleotide "8A" and an all RNA version constitute the two sense oligos used in this study; the other three oligos are the antiattenuator fragments. (B) Initial cleavage rates for single-turnover reactions for various ribozyme−oligonucleotide combinations. Ribozymes are denoted below the plots: black bars, no activating oligonucleotide; gray bars, activated with sense DNA oligo 8A; white bars, activated with RNA versions of sense oligo 8A; and diagonally striped bars, activated with DNA oligos that include antiattenuator sequences (8A+6 through 8A+10). Error bars indicate the standard deviations of three to five measured values. Numbers above the bars represent the relative enhancement of observed cleavage rates within each group relative to the reaction of that ribozyme without the activating oligo.

serve as a powerful modulator of ribozyme kinetics (*1*). To exploit this fact, allosteric hammerhead ribozymes were designed to cleave a target RNA strand upon activation by exogenous RNA or DNA following the TRAP design. "Antisense" and "attenuator" sequences were appended onto the catalytic core of a hammerhead known to display simple kinetic behavior. Pairing of the attenuator with the core should interfere with hammerhead activity, defining the off state for the ribozyme (Figure 2, left). The duplex formed by interaction of a "sense" oligonucleotide with the antisense portion of the construct should form a stable helix that competes with binding of the attenuator to the core, thereby activating the hammerhead to cleave its substrate (Figure 2, right).

Hammerhead HH8 was chosen as the structural core because it displays simple monophasic kinetics for single-turnover cleavage of a small RNA substrate (*22*), suggesting that chemistry, and not structural rearrangement, is normally rate-limiting. Using a short, radiolabeled oligoribonucleotide for the cleavage substrate, we observe an apparent first-order rate constant (k_{obs}) of 0.6 ± 0.1 min^{-1} for the parental HH8, which is similar to the published value of 1.0 min^{-1} (*22*). Hammerhead HH8A, composed of the HH8 core with a 20-nucleotide, A-rich antisense extension on its 3′ end (Figure 3A), gave an indistinguishable rate ($k_{obs} = 0.63 \pm 0.02$ min^{-1}, Figure 3B). Thus, the A-rich antisense region does not interfere with hammerhead function, and presumably does not base pair with other portions of the ribozyme.

To shut down substrate cleavage activity, attenuator sequences of varying lengths were appended onto the 3′ ends of the antisense segment. The attenuators are designed to base pair with the conserved catalytic core and with a portion of stem II (Figure 3A). Both arms of the IGS remain intact, and these ribozymes are presumed to retain substrate binding activity. A ribozyme with a six-nucleotide attenuator, termed HH8A.6, exhibited a marginally decreased single-turnover cleavage rate. In contrast, ribozymes with longer attenuators exhibited single-turnover cleavage rates that were 300- to >1000-fold suppressed relative to HH8A (Figure 3B). The six-nucleotide attenuator appears to be unable to compete with the native ribozyme structure, while the longer attenuators likely force an inactive, alternative structure by pairing with the catalytic core as in Figure 2.

Sense Oligonucleotides Restore Cleavage Activity through Sense−Antisense Interaction. To assess whether sequestering the antisense portion would activate these TRAP ribozymes, DNA oligonucleotide "8A" (complementary to the A-rich antisense segment shown in Figure 3A) was added to each ribozyme prior to folding in the presence of substrate. Reactions with HH8A, HH8A.6, and HH8A.8 all exhibited similar rates in the presence of oligo 8A, and these rates were comparable to the rate observed for hammerhead HH8 alone (Figure 3B). Stimulation of the cleavage rate upon addition of sense oligonucleotide 8A to HH8A.8 is most dramatic, activating this ribozyme nearly 200-fold. The cleavage rate observed for ribozyme HH8A.10 is also enhanced by addition of 8A, although only 15-fold above the unactivated rate. Thus, its activity is still far below the rates seen for the unattenuated ribozyme.

We hypothesize that the failure to achieve complete rescue of HH8A.10 using the sense DNA reflects the relative stabilities of the two competing helices: a 10-nucleotide GC-rich, intramolecular RNA−RNA helix on one hand (between attenuator and core) versus a 20-nucleotide AT-rich, intermolecular RNA−DNA helix on the other (between antisense and sense). To push the equilibrium toward formation of the 20-nucleotide antisense−sense helix, an RNA version of the 8A sense oligo was used in place of DNA to activate the ribozymes, as RNA−RNA helices are more stable than RNA−DNA helices (*5*, *23*−*26*). Use of the RNA sense oligo gave dramatic results for HH8A.10, for which the measured value of k_{obs} (0.13 ± 0.08 min^{-1}) is 260-fold higher than

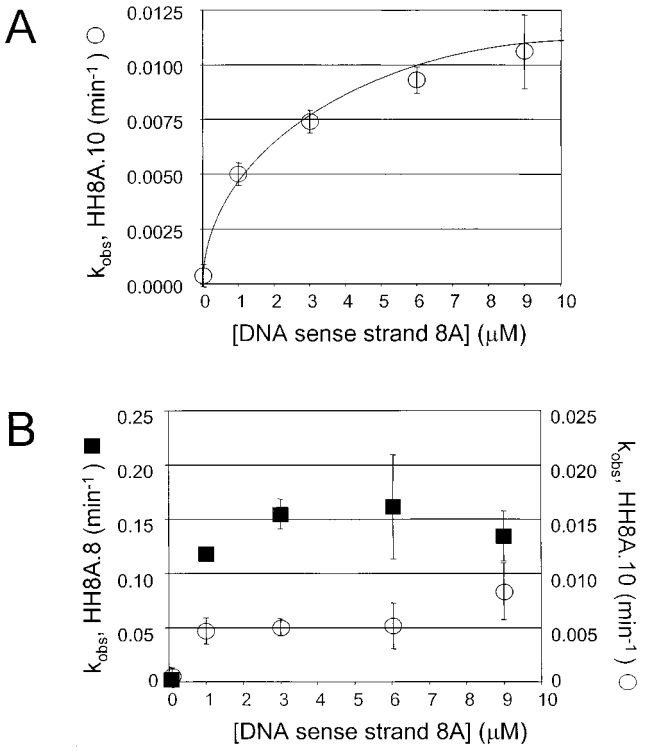

FIGURE 4: Effect of the concentration of the DNA sense oligo on cleavage rates of attenuated ribozymes. (A) The sense oligo was added to HH8A.10 RNA prior to folding the ribozyme with the substrate, and reactions were initiated by adding Mg^{2+}. Data were fit to a standard saturation curve. (B) Ribozyme−substrate complexes of HH8A.8 (■) or HH8A.10 (○) were annealed, and then the sense oligo was added along with Mg^{2+} to initiate reaction. The vertical axis for HH8A.8 is on the left side of the plot, and the vertical axis for HH8A.10 is on the right. Error bars in both plots reflect standard deviations of four measurements of k_{obs}.

the unactivated rate. HH8A.8 was similarly activated by the RNA sense oligo, exhibiting a cleavage rate (0.65 ± 0.02 min^{-1}) that is 270-fold greater than that seen for the unactivated form. HH8A and HH8A.6 were already near their maximal rates, and did not distinguish sharply between RNA and DNA sense oligos.

If formation of the sense−antisense helix is rate-limiting for the attenuated ribozymes, then altering the concentration of sense oligo should influence the observed rate of substrate cleavage by shifting this equilibrium. The assays described above were carried out using 3 μM 8A, 1 μM ribozyme, and 0.1 μM substrate to ensure that the ribozyme was in stoichiometric excess of the substrate, and that the activating sense oligo was in excess of the ribozyme. To test the effects of altering the concentration of the DNA sense oligo, this component was varied from 1 to 9 μM (Figure 4A). Over this 9-fold range, the cleavage rates observed for HH8A.10 nearly doubled, consistent with a steady shift in the ribozyme's internal structural equilibrium. Furthermore, the data can be readily fit to a standard saturation curve with a half-maximal value for k_{obs} at 1.8 ± 0.3 μM sense DNA. These data and those in Figure 3B demonstrate that hammerhead ribozymes can be turned off by inclusion of an attenuator sequence, and that they can activated by a sense oligo.

Alternative Modes of Oligonucleotide-Mediated Allostery. In the activation noted above, the sense oligonucleotides are designed to interact only with the antisense portion of the ribozyme without directly pairing with any of the attenuating nucleotides. In parallel experiments, attenuated ribozymes were incubated with DNA sense oligos that also included an antiattenuator sequence on their 5′ ends (Figure 3A, top left). To maintain a fixed length of 20 nucleotides, the activating oligos were correspondingly shortened at their 3′ ends in the sense portion. Antiattenuator oligo "8A+6", for example, carries 14 nucleotides of sense sequence and six nucleotides complementary to the attenuator, and was used in conjunction with hammerhead HH8A.6. When the three attenuated ribozymes were folded in the presence of their corresponding antiattenuator oligos, cleavage activity for each combination was similar to that observed for HH8 (0.8−0.9 min^{-1}) (Figure 3B). These values correspond to 360- and 1760-fold increases in the apparent rates of cleavage for HH8A.8 and HH8A.10, respectively. As the observed cleavage rates are indistinguishable from the rate observed with the nonattenuated parental ribozyme, no further activation appears to be possible.

Order of Addition Suggests both Thermodynamic and Kinetic Competition among Alternative Structures. In the cleavage assays described above, the ribozymes, substrates, and activating oligos were all present together during the unfolding and refolding reactions. For some analytical or intracellular applications, it might be advantageous to allow the attenuated precleavage complex to assemble and remain relatively inert until activated by an exogenous RNA or DNA species. To determine whether sense oligos can activate preassembled, attenuated ribozymes, ribozyme HH8A.8 was folded with substrate but without divalent ions. DNA sense oligo 8A was folded separately in the presence of Mg^{2+}, and the cleavage reaction was initiated by mixing the two solutions. As shown in Figure 4B, the observed rate of cleavage by HH8A.8 is significantly higher (~50-fold) than in the absence of the activating oligo. However, this is ~1/4 of the cleavage rate seen when the oligo is added during the folding step (compare to Figure 3B). A similar pattern was observed for HH8A.10, which exhibits 10-fold activation after the HH8A.10 complex had already assembled, versus 16-fold activation when the oligo was added prior to folding. Thus, while both ribozymes were stimulated by addition of the sense oligo after folding, the degree of stimulation was slightly lower if the attenuated complex had already formed.

The order-of-addition experiment described above does not account for any Mg^{2+}-dependent stabilization of the attenuated complex that might interfere with association of the sense strand. Therefore, cleavage reactions by HH8A.8 and HH8A.10 were monitored before and after the sense oligo was added to the reaction mixtures. Both ribozymes cleaved the substrate RNA faster after the sense oligo was added than before it was added (compare the slopes in Figure 5A), though the degree of stimulation was <10-fold under these conditions (Figure 5B). Similar reactions were carried out using the antiattenuator oligos 8A+8 and 8A+10. While these oligos stimulated the reaction much more strongly than did the sense oligos (59- and 152-fold, respectively), the degree of stimulation is again reduced by ~10-fold relative to that observed when the oligo was added before the folding step. The attenuated complex may thus form a kinetic folding trap that impedes equilibration with the activating oligo (although this possibility was not tested directly with diluted denaturants). Optimal design of activatable ribozymes should

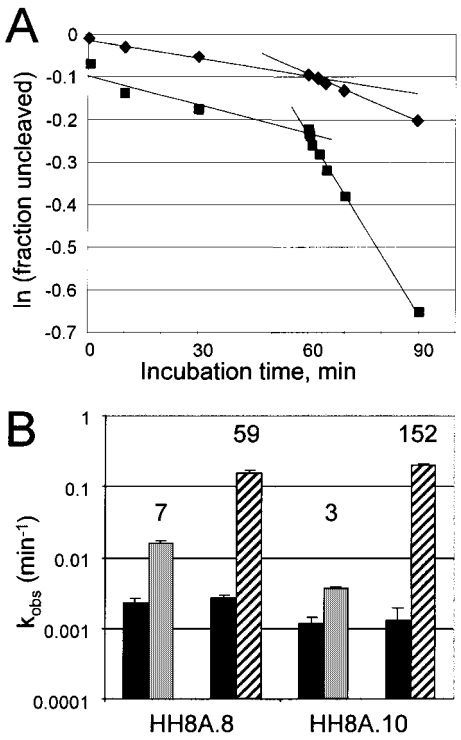

FIGURE 5: Stimulation of attenuated ribozymes after the cleavage reaction has begun. (A) Representative time course showing the natural logarithm of the uncleaved fraction of a radiolabeled RNA substrate vs time for HH8A.8 (■) and for HH8A.10 (◆). Best-fit lines are shown for rates of cleavage before and after addition of the activating DNA sense oligo at 1 h. (B) Activities of HH8A.8 and HH8A.10 before (black bars) and after addition of either sense (gray bars) or antiattenuator (diagonal stripes) activating DNA sense oligo. Prestimulation cleavage rates were averaged over the course of 1 h (poststimulation for 3 min). Error bars reflect standard deviations of three to four separate trials. Numbers above the bars indicate the fold increase in the observed rate of cleavage upon addition of oligo, relative to the rate observed prior to oligo addition.

thus incorporate not only the thermodynamic stabilities of the equilibrium structures but also the kinetic ability of the activating species to gain access to the attenuated RNA.

DISCUSSION

Allosteric Regulation of TRAP Ribozymes. The primary aim of this work was to determine whether the RNA cleaving activity of hammerhead ribozymes could be regulated in an allosteric manner that did not require the attenuating sequence to be recognized by the sense strand. The data in Figures 3−5 show that such regulation is indeed possible. Two different attenuated ribozymes exhibited >250-fold activation by RNA sense oligonucleotides, making this strategy comparable to several other regulation strategies (vide infra). The complete system involves three RNA or DNA molecules: the ribozyme, its cleavage substrate, and the activating species. In the "closed" form of the ribozyme, an appended sequence ("attenuator") that binds to the catalytic core prevents formation of the active structure. This attenuated form must compete with the normal folding of the core. The six-nucleotide stem that could form between the attenuator and core in HH8A.6 seems to be too weak to compete with the structural integrity of the folded core, based on the observation that HH8A.6 exhibits nearly full activity. Note that four of the six pairs for this attenuator would compete directly with formation of stem II. In contrast, the 8- and 10-nucleotide attenuators in HH8A.8 and HH8A.10 repress RNA cleavage activity much more effectively. The "open" form of the ribozyme is generated when the activating species anneals with an antisense segment between the ribozyme core and the attenuator. This annealing event forces the duplex between the attenuator and core to melt, allowing the ribozyme to fold into its active conformation.

Three lines of observation support the hypothesis that activation in the HH8A series is due to competition among alternative structures. The first is that increasing the concentration of the activating DNA oligo prior to folding augmented the degree of activation (see Figure 4A). LeChatlier's Principle dictates that more of the sense−antisense duplex should form as additional sense oligo is added. HH8A.10 shows apparent saturation kinetic behavior for the activating DNA sense oligo, with half-maximal activation for the interaction at 1.8 ± 0.3 μM DNA. While this aspect of the stimulation was not examined in detail, it may reflect the K_m or K_d for the binding of the sense oligo to the attenuated ribozyme. In isolation, the sense−antisense interaction is expected to have a much lower K_d. The $\Delta G°$ for formation of the same helix in the context of an attenuated ribozyme, on the other hand, will necessarily include unfavorable free energy terms due to disruption of the stem between the attenuator and core, forcing the K_d value to be higher that what might be observed for the helix in isolation.

The second observation supporting the competitive model for the mechanism of activation is that an RNA oligonucleotide provided greater activation than that observed for a DNA oligonucleotide. The three HH8A.10 reactions (unactivated, DNA-activated, and RNA-activated) gave k_{obs} values of 0.0005 ± 0.0001, 0.0074 ± 0.0005, 0.13 ± 0.08 min^{-1}, respectively. Assuming that the rate-limiting step in each case is the conformational rearrangement, and setting the difference in the free energies of activation, $\Delta\Delta G^{‡} = -RT \ln(k_{obs,activated}/k_{obs,attenuated})$, we find the DNA and RNA oligos provide -1.6 and -3.3 kcal/mol, respectively, toward accelerating the reaction. The additional -1.7 kcal/mol obtained from using the RNA sense strand instead of DNA could derive from the known increase in the stability of RNA−RNA helices relative to RNA−DNA hybrids (*5*, *23*−*26*). Using tabulated thermodynamic parameters for helix formation (*25*), we calculate that the antisense−sense duplex in this study is 0.65 kcal/mol more stable as an RNA−RNA helix than as a DNA−RNA hybrid. While the experimental and calculated $\Delta\Delta G^{‡}$ values are in close agreement, the thermodynamic values were tabulated for a standard state of 1 M Na^+ and no Mg^{2+} at 37 °C, and the cleavage experiments outlined here were carried out at 25 °C in 10 mM Mg^{2+} with no Na^+, making it difficult to compare the numbers directly. It will be important to measure ΔG values directly under the conditions used in the kinetic assays. Nevertheless, the observations fit the qualitative expectations based on known relative helical stabilities, and they are in reasonable agreement with quantitative predictions.

The third observation supporting the competitive model lies in the biphasic kinetics exhibited by HH8A.8 (see Figure 5A). It can be assumed that some fraction (f_a) of the ribozyme molecules forms the attenuator−core helix and is repressed while another fraction ($1 - f_a$) bypasses the attenuator and folds directly into the active conformation. Upon addition of Mg^{2+}, an initial burst should be observed during which

pr-folded molecules cleave their targets, and then subsequent cleavage will be limited by the rate of conformational change that spontaneously releases the attenuator−core interaction. This is precisely the behavior seen for HH8A.8, which carries an eight-nucleotide attenuator (see Figure 5A). For this ribozyme, ~13% of the molecules cleave within the first 10 min, while only an additional 7% cleave over the subsequent 50 min. Ribozymes HH8A.6 (not shown) and HH8A.10 (Figure 5A) give monophasic kinetics. As noted above, ribozyme HH8A.6 appears to fold almost completely into the active conformation so that chemistry remains rate-limiting through the reaction. The 10-nucleotide attenuator of ribozyme HH8A.10, on the other hand, allows the inhibitory helix to form in an overwhelming majority of the molecules, making conformational change rate-limiting throughout the reaction.

Design Features for Practical Applications. The mutually exclusive alternative conformations that define the open and closed states of the TRAP are in competitive equilibrium. Optimal probe design requires a careful balance among the factors that shape this equilibrium. The attenuating stem should be stable enough to minimize transient melting of the helix that could result in an elevated background. The antisense loop must be large enough that the antisense−sense helix is more stable than the self-structure in the probe so that it can disrupt the attenuated structure. At the same time, the antisense regions would ideally be short enough to remain sensitive to mismatches to allow discrimination among alleles or multiple loci of a given target.

In principle, the TRAP design can be adapted to utilize almost any structurally accessible RNA or DNA to activate cleavage of a target RNA. There is no requirement for either the activating sequence or the antisense to inhibit the ribozyme directly. On the other hand, such interaction should not present a problem, so long as it can be overcome by annealing to the sense RNA or DNA species. In the work presented here, much greater stimulation for all attenuated ribozymes was observed when the activating oligos targeted the attenuator sequences directly (striped bars in Figure 3B). For HH8A.10, this amounted to 1760-fold more cleavage activity in the presence of the DNA oligo than without the activator. In this mode of activation, there is essentially no distinction made between the antisense and attenuator, because the appended sequence must interact both with the ribozyme core and with the activating RNA or DNA strand. From a general design point of view, however, using the antisense to attenuate the ribozyme places stringent limitations on sequence choice. Specifically, the sequence that will be used to activate the ribozyme must be chosen such that its complement interferes with the ribozyme. However, the antiattenuator data also suggest that greater stimulation may be possible using longer antisense segments, or sequences that form more stable interactions with the sense strand than the interactions observed with the poly(A) sequence used here.

TRAP Design versus Other Regulatory Designs. Several strategies have been devised to regulate substrate cleavage activity by RNA and DNA enzymes with exogenous effector molecules. While detailed kinetic analyses have only been carried out for some, each is likely to reversibly perturb one or more of the precleavage equilibria shown in Figure 1. Ribozymes and DNAzymes have been devised that respond to small molecule effectors (*10*−*16*), specific metal ions (*17*), or proteins (*18*), and they are being recruited for the development of sensitive and specific biosensors (*19*, *27*−*29*). Binding of the effectors is generally believed to stabilize a helix in the enzyme (especially stem II for allosteric hammerheads), allowing the active conformation to form. In the context of the kinetic scheme in Figure 1, the $K_{E\cdot S}$ equilibrium is the point of regulation because while the IGS remains accessible to bind the substrate, the enzyme−substrate complex is unable to achieve its active conformation. Addition of the effector then shifts the E·S′ ⇔ E·S equilibrium toward formation of the active E·S complex. In some cases, effector binding may also directly influence substrate binding.

Ribozymes and DNAzymes that respond to oligonucleotide effectors have also been isolated (*4*−*9*), though their mechanisms of regulation differ markedly from that presented here. One strategy uses the activating oligo to stabilize an otherwise unstable structure in any of several kinetic steps. For example, in the "expansive" regulation of a DNAzyme described by Wang and Sen, substrate binding is made dependent upon the presence of an RNA or DNA effector. In this system, the IGS is mostly replaced with sequences that bind to part of an activating RNA or DNA species (*5*) (antisense). The activating species also binds flanking sequences in the cleavage substrate. Although the short IGS−substrate stem does not support productive substrate binding, formation of the three-way junction stabilizes the active complex. This strategy thus targets k_1 by turning substrate binding into a multistep binding process. In another example, Komatsu et al. replaced stem II of a hammerhead ribozyme with a large loop of defined sequence (*6*). They then added an oligonucleotide that bound to sequences along one side of the loop, forming what they describe as a half-pseudoknot. The new stem stacks onto the core, stabilizing the active conformation and shifting K_E to favor the active fold of the enzyme.

In contrast, the inactive states for other regulated (deoxy)-ribozymes are formed by stabilization of alternative structures. These ribozymes carry sequence elements that suppress activity in analogy with the attenuators described here unless they are directly sequestered by an added oligonucleotide. This was an accidental feature of a self-phosphorylating ribozyme (*7*) and a ligase ribozyme (*8*), for which oligos used during their selections are postulated to prevent the formation of the alternative structures. Even so, the ligase ribozyme was activated 1000−10000-fold by addition of appropriate oligos (*8*). For both the self-phosphorylating ribozyme and the ligase, removal of the attenuating nucleotides restored essentially full activity (refs *7* and *8* and unpublished observations of S. Rhee, K. Woodard, S. Jain, and D. Burke). As described above, direct activation by disruption of inhibitory interactions is a powerful strategy when it can be used, but its general application is extremely limited because of the tight constraints imposed upon the sequence to be detected. The "maxizymes" of Kuwabara et al. (*30*−*33*) constitute another example in which alternative structures suppress ribozyme activity. These maxizymes are hammerhead derivatives that cleave a portion of the BCR-ABL mRNA, but they have been engineered to assemble the active ribozyme only when a built-in antisense segment anneals with a second binding site in the target RNA

(*30*). The antisense portion joins the two arms of the IGS (stems I and III). When not bound to its sense target, it is thought to promote the formation of alternative, inactive conformations that prevent substrate binding at the IGS. Thus, even though it does not bind directly to the catalytic core, the antisense is again serving a dual role as attenuator. The maxizyme system is highly complex, and it is not yet clear how easily this strategy can be adapted to new systems.

Conclusion. The TRAP design described in this work represents a new mode of allosteric regulation of RNA-cleaving ribozymes. There are no fundamental constraints on the choice of antisense sequence, and this strategy should be readily generalizable to a broad range of cleavage substrates, to activating RNAs, and even to ribozymes with activities other than RNA cleavage. Even without extensive rational design or exploiting the evolutionary optimization in vitro, we observe a more than 250-fold rate enhancement for the single-turnover cleavage reaction. The limiting extent of activation is likely to be proportional to the ratio of relative stabilities of the sense−antisense helix with the folded core to the attenuator−core helix. It should be possible to maximize this ratio through rational design or through evolutionary optimization. One possible application of this strategy is for enzyme-linked or chip-based analyte detection. Another is to use the sense−antisense interaction to query the physiological state of a cell. If RNAs associated with viral infection or oncogenesis are detected, the ribozyme can cleave an mRNA from a reporter gene such as luciferase or one that encodes a protein required for cell survival.

ACKNOWLEDGMENT

We thank Dr. Evelyn Jabri and members of both our labs for comments on the manuscript.

REFERENCES

1. Stage-Zimmermann, T. K., and Uhlenbeck, O. C. (1998) *RNA 4*, 875−889.
2. Narlikar, G. J., Khosla, M., Usman, N., and Herschlag, D. (1997) *Biochemistry 36*, 2465−2477.
3. Thirumalai, D., and Woodson, S. (2000) *RNA 6*, 790−794.
4. Porta, H., and Lizardi, P. M. (1995) *Biotechnology 13*, 161−164.
5. Wang, D. Y., and Sen, D. (2001) *J. Mol. Biol. 310*, 723−734.
6. Komatsu, Y., Yamashita, S., Kazama, N., Nobuoka, K., and Ohtsuka, E. (2000) *J. Mol. Biol. 299*, 1231−1243.
7. Lorsch, J. R., and Szostak, J. W. (1995) *Biochemistry 34*, 15315−15327.
8. Robertson, M. P., and Ellington, A. D. (1999) *Nat. Biotechnol. 17*, 62−66.
9. Stojanovic, M. N., de Prada, P., and Landry, D. W. (2001) *Chembiochem 2*, 411−415.
10. Piganeau, N., Thuillier, V., and Famulok, M. (2001) *J. Mol. Biol. 312*, 885−898.
11. Araki, M., Hashima, M., Okuno, Y., and Sugiura, Y. (2001) *Bioorg. Med. Chem. 9*, 1155−1163.
12. Jose, A. M., Soukup, G. A., and Breaker, R. R. (2001) *Nucleic Acids Res. 29*, 1631−1637.
13. Robertson, M., and Ellington, A. (2000) *Nucleic Acids Res. 28*, 1751−1759.
14. Koizumi, M., Soukup, G. A., Kerr, J. N., and Breaker, R. R. (1999) *Nat. Struct. Biol. 6*, 1061−1071.
15. Araki, M., Okuno, Y., Hara, Y., and Sugiura, Y. (1998) *Nucleic Acids Res. 26*, 3379−3384.
16. Tang, J., and Breaker, R. R. (1997) *Chem. Biol. 4*, 453−459.
17. Li, J., Zheng, W., Kwon, A. H., and Lu, Y. (2000) *Nucleic Acids Res. 28*, 481−488.
18. Robertson, M. P., and Ellington, A. D. (2001) *Nat. Biotechnol. 19*, 650−655.
19. Frauendorf, C., and Jaschke, A. (2001) *Bioorg. Med. Chem. 9*, 2521−2524.
20. Mulligan, J. F., and Uhlenbeck, O. C. (1989) *Methods Enzymol. 180*, 51−62.
21. Soukup, G. A., DeRose, E. C., Koizumi, M., and Breaker, R. R. (2001) *RNA 7*, 524−536.
22. Fedor, M. J., and Uhlenbeck, O. C. (1990) *Proc. Natl. Acad. Sci. U.S.A. 87*, 1668−1672.
23. Hall, K. B., and McLaughlin, L. W. (1991) *Biochemistry 30*, 10606−10613.
24. Lesnik, E. A., and Freier, S. M. (1995) *Biochemistry 34*, 10807−10815.
25. Sugimoto, N., Nakano, S., Katoh, M., Matsumura, A., Nakamuta, H., Ohmichi, T., Yoneyama, M., and Sasaki, M. (1995) *Biochemistry 34*, 11211−11216.
26. Gray, D. M. (1997) *Biopolymers 42*, 795−810.
27. Seetharaman, S., Zivarts, M., Sudarsan, N., and Breaker, R. (2001) *Nat. Biotechnol. 19*, 336−341.
28. Kuwabara, T., Warashina, M., and Taira, K. (2000) *Curr. Opin. Chem. Biol. 4*, 669−677.
29. Stojanovic, M. N., de Prada, P., and Landry, D. W. (2000) *Nucleic Acids Res. 28*, 2915−2918.
30. Kuwabara, T., Hamada, M., Warashina, M., and Taira, K. (2001) *Biomacromolecules 2*, 788−799.
31. Kuwabara, T., Warashina, M., and Taira, K. (2000) *Trends Biotechnol. 18*, 462−468.
32. Tanabe, T., Kuwabara, T., Warashina, M., Tani, K., Taira, K., and Asano, S. (2000) *Nature 406*, 473−474.
33. Kuwabara, T., Warashina, M., Tanabe, T., Tani, K., Asano, S., and Taira, K. (1998) *Mol. Cell 2*, 617−627.

BI0201522